The International Journal of Engineering and Science (IJES)
|| Volume || 14 || Issue || 1 || Pages || PP 04-21 || 2025 ||
ISSN (e): 2319 – 1813 ISSN (p): 2319 – 1805

Differences for Cooling Capacity of a Cable Tunnel System: Install One or Three Additional Cable Troughs with Cable Circuit for 100/70 Heat Loads – A Numerical Study

Steven[1] and Chen Xiaobing[1]
[1]*The University of Newcastle, Australia*
Corresponding Author: steven@uon.edu.sg

----------ABSTRACT----------
The purpose of this report was to compare the numerical analysis for different cooling efficiency of a cable tunnel system when installing one additional cable trough or three cable troughs for cable circuit 100% or 70% heat load. Cable tunnel system is widely known for it is use for high voltage transmission in an underground. Due to the cables generating large quantities of heat, water pipes and air ventilation were used in the tunnel to cool down the transmission cable. To investigate the cooling efficiency of a tunnel, research for benchmark case was carried out. A Computational Fluid Dynamic (CFD) benchmark analysis about 2D natural convection inside the square cavity was investigated to further understand the air movement inside the square medium. Ansys Fluent was carried out for benchmark cases of heat transfer natural convection inside the square cavity and to check whether Ansys Fluent can be used for any CFD and heat transfer purposes by validating the results with previous studies. The benchmark case used a 2D square with different active temperature side walls and adiabatic walls for top and bottom side. From the benchmark simulations with different Rayleigh Number, a number representing buoyancy-driven of a fluid from 10^3 to 10^5 affected air differently and the heat transfer natural convection inside the square. At different Rayleigh Number air forms a recirculation passing the active walls and adiabatic walls. After investigated the benchmark, the results were used to validate with previous studies. To validate the results was by using Nusselt Number, ratio of convective to conductive. The benchmark case results were validated and Ansys Fluent proven can be used for CFD and heat transfer purposes. Two 3D cable tunnel were modelled with 100-meter length after concluded the benchmark. The two tunnel models were based on the number of cable troughs installed. The first tunnel was with one cable trough and two cable circuits on the bottom, as for the second tunnel was with one bottom cable circuit and three cable troughs. Cable tunnel simulations were based on cable circuit for 100% heat load and 70% heat load with each heat load case was given different water flow rate of 4.25 L/s and 6.5 L/s. A total of eight scenario cases were carried out to determine which provided a better cooling efficiency choice. The analysis for cable tunnel cases on how the copper cables cooled down through heat transfer of natural convection inside the cable trough, which the heat then was removed from the cable circuit by air and continue to the outside of the tunnel. During the heat transfer processes, conductivity was present as not all heat were removed by air and water, but continue to through the walls of the tunnel and to the ground soil. Based on the simulations, a cable tunnel with three cable troughs was proven more cooling efficiency compared tunnel with one cable trough. Some scenarios did not meet the criteria, due to insufficient heat relocation by air and water. The cooling efficiency was determined by which has the better balance heat relocation by air, water, and ground, also considering the comfort and safety of human inside the tunnel.

KEYWORDS; - *Cable tunnel system, natural convection, and Computational Fluid Dynamic.*

Date of Submission: 27-12-2024 Date of acceptance: 07-01-2025

I. INTRODUCTION

Cable tunnel system is an underground electricity cable used for transmit a high voltage of electrical power for a long distance. Tunnel system was used to provide the power distribution, data communication, and transport infrastructure for commercial, industrial, and residential usage. The cable tunnel system is located underground due to cables extending several kilometers, minimizing the used of space, and reducing visual impacts of cables if it is in public areas. Since the cable tunnel generates heat from transmitting power at high voltage, to prevent failure of the cable due to overheat, air ventilations and water tunnel pipes are required in the

tunnel to cool down the temperature of the cable. The environmental surrounding of the cable when performing heat exchange can also affect the temperature of a soil and surrounding air. The 3D Computational Fluid Dynamic (CFD) modelling design for the cable tunnel with the use of Ansys and require the process of the heat transfer in the tunnel can be examine through the modelling and simulations. For a standard CFD modelling tunnel ventilation design, the modelling of the 3D for the cable tunnel must be accurately exact as intended to obtain an accurate result. Things to consider are the aerodynamic phenomena in the tunnel, boundary conditions, and the geometry. Due to the limitation of the computer that used to perform the simulation and analysis for the cable tunnel system, the geometry of the tunnel and cable was simplified with length of 100 meter.

II. LITERATURE REVIEW

Due to the cable tunnel system transmit through cables at a high voltage producing a large quantity of heat, a cooling from the air ventilation is needed to remove the heat. When air enters from the ventilation to heat exchange with the cables when transmitting power, the air temperature increases along the length of the cable tunnels until it leaves the tunnel. Davies, Revesz, and Maidment (2019) used methods such as Cold Led Head Recovery (CLHR) system and Heat Lead Heat Recovery system (HLHR) to cool the tunnel temperature [1-6]. The CLHR method using the air to heat exchange with the water at the end of the ventilation system. While the HLHR method is at the exhaust ventilation shaft, it however does not provide cooling for the electrical cables. But depends on the air ambient temperature and the applied temperature can change the result but the two methods were able to recover of heat. Example of a cable tunnel design from Singapore located 2.6 km undersea by Jensen and Adi-Zadeh (1988), the heat generated by the power was removed by the cooling water system and a ventilation system through heat transfer calculations and basis for structural stress analysis. A 100 meters long tunnel with the maximum cable loading of power station at 2000 MVA and 230 kV with seven cable circuit designed for 500 MVA [7-10] are arranged in flat for the power circuit and cooling pipes cover with lean mix concrete with a thermal conductivity of 0.8 W/m K for each cable producing different heat, with four cables generating 365 W/m heat, one cable generate of 89 W/m, and two cables generating 181 W/m. The method that was used for cooling the heat of a cable was with the water-cooling system, by having each power circuit linked to two piped cooling water circuits with each pipe has a water flow rate of 3 kg/s at a maximum outlet temperature of 40 ℃. and second method the tunnel ventilation using the environment to control the tunnel atmosphere by installing six axial flow, vertical mounted, two speed, two stage, contra rotating [11-19], reversible fans. Regarding to a multi-scale analysis for a Utility tunnel the design of the tunnel divided into three or four compartments to contain pipelines with different hazard levels. The compartment has fire-rated walls and isolated zones doors. Accommodation of the tunnel consist multiple utilities such as water, sewerage, gas, electrical power, telephone, and heat supply. As the utility tunnels meant for sustainable development of cities [20-31], fire problem has not been focused on for a long time. Despite not enough attention of the fire problem, the ventilation system is expected guarantee the safety of the pipelines, fire fighters, and structures.

When heat is transferred through the movement of a heated fluid or gas this phenomenon heat transfer is called convection. In convection energy is redistributed from hotter areas to cooler areas. Convection heat transfer can be a natural convection and forced convection [32]. The heat exchange change of temperature within the cable trough from a cable tunnel system is the natural convection due to the fluid movement from air temperature surrounding the cable to go upward direction due to a buoyancy force. Natural convection is a heat transfer between a solid and moving fluid or gasses such as water or air with different temperature for a heat to move that occurs by natural causes such as buoyancy. Buoyancy force is the upward force applied from a fluid on a body by completely or partially. Natural convection mechanism of heat transfer is applicable for cooling of electronic equipment such as power transistors or the main case of the cable tunnel is the heated cable. As an object with high temperature is exposed to a cold air, the temperature [33-40] outside of the object have a heat transfer with the cold air causing the outside temperature to decrease and the air temperature near the object increases. As the motion of the heated air temperature near object causing the lower density for the air, this motion is called the natural convection current. Without the current or the buoyancy force the heat transfer would be considered as conduction rather than convection.

Natural convection in square cavity is the natural convection of heat transfer in a square close confined space due to temperature differences causing a heat transfer through buoyancy forces. This natural convection involves the Navier-Stokes equations, where the fluid with solid wall or no-slip boundary condition. The top and bottom sides of the square are assumed in adiabatic or perfectly insulated. The left side of the square is considered as cold temperature and while the right side as the hot temperatures causing the air inside of the cavity to experience change of temperature and behavioral. Previous case of study on natural convection inside a square cavity has been conducted by many scientific researchers in engineering to improve cooling of electronics. Numerical study for natural convection of air inside square cavity with partially thermally active side walls by

Kane, Mbow, Sow, and Sarr (2017) [41-45] shows that different heights of velocity values and temperature can be fluctuated by convection and cause the air movement to go upward and downward. The contours of velocity vector maps have the existence of stagnant zone in the center of cavity indicating a heat exchange in an intense way at the corners of cavity with the fluid particles move greater at locations of the wall that has active temperature and less movements in the adiabatic side of the wall.

Effect of fluid-structure interaction on transient natural convection in an air-filled square cavity by A. Raisi and i. Arvin (2018) stated that the increase of Rayleigh number [46-48] can affects the interaction of fluid and structure and strengthens the natural convection inside the cavity. This study uses an object of thin deformable baffle located horizontally in center of the square cavity. The length of the baffle provides different results of the thermal performance in cavity depends on the Rayleigh number [49-54], as the baffles increase in length at low Rayleigh number weakens the natural convection and reduces the average Nusselt number. However, high Rayleigh number with the increase length of the baffle resulting a strong vortex and increase of average Nusselt number.

III. INVESTIGATE THE BENCHMARK CASE

Investigate the natural convection inside a square cavity through Computation Fluid Dynamics (CFD) with the use of Ansys. Natural convection inside the square cavity on the heated region and cold region of the walls at different Rayleigh number can affects convection of the air fluid. Air was used as fluid in this benchmark to study the natural convection by the buoyancy force and how the airflow affected towards temperature differences. Dimensionless number of Nusselt number was used for validation results since it is ratio of convection and conduction heat transfer. Results of this experiment were to be compare with previous studies to validate the results and determine whether Ansys fluent provides accuracy that can be used for heat transfer and CFD modelling. Through Ansys Workbench [55-61], Ansys fluent was used for the study of 2D natural convection inside the square cavity. Geometry was set at 2D to create the computational model for square shape geometry with dimensions of 1 x 1 meters and mesh of 82 x 82 was generated for element size of 0.01 m with each edge side of the geometry were given edge sizing mesh to make it denser. Figure 1 shows how the square geometry with mesh generated look like.

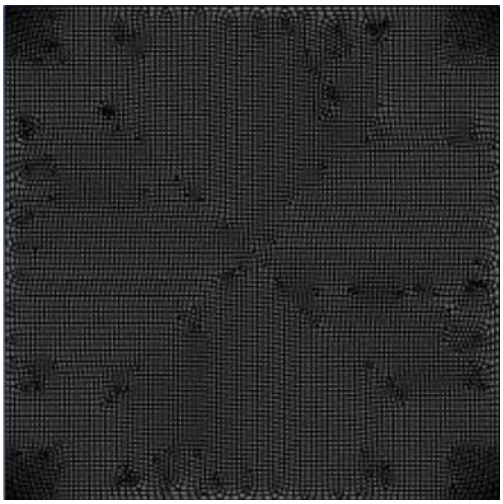

Figure 1 The square cavity setup

To analyze the benchmark case was by through with three simulation scenarios based on the different temperature from the hot temperature wall value and this simulation was related to the Rayleigh number, a number associated with buoyancy-driven of a fluid. Table 1 is the list of different scenarios case were carried out for the simulation benchmark.

Table 1 List of scenario case for benchmark.

Rayleigh Number	Hot wall temperature (K)
1000	14.1723356
10000	141.723356
100000	1417.23356

The simulations were run with 1000 number of iterations using SIMPLE method and assumed with no-slip wall conditions. After run the simulations, results were analyzed and discussed the airflow inside the cavity.

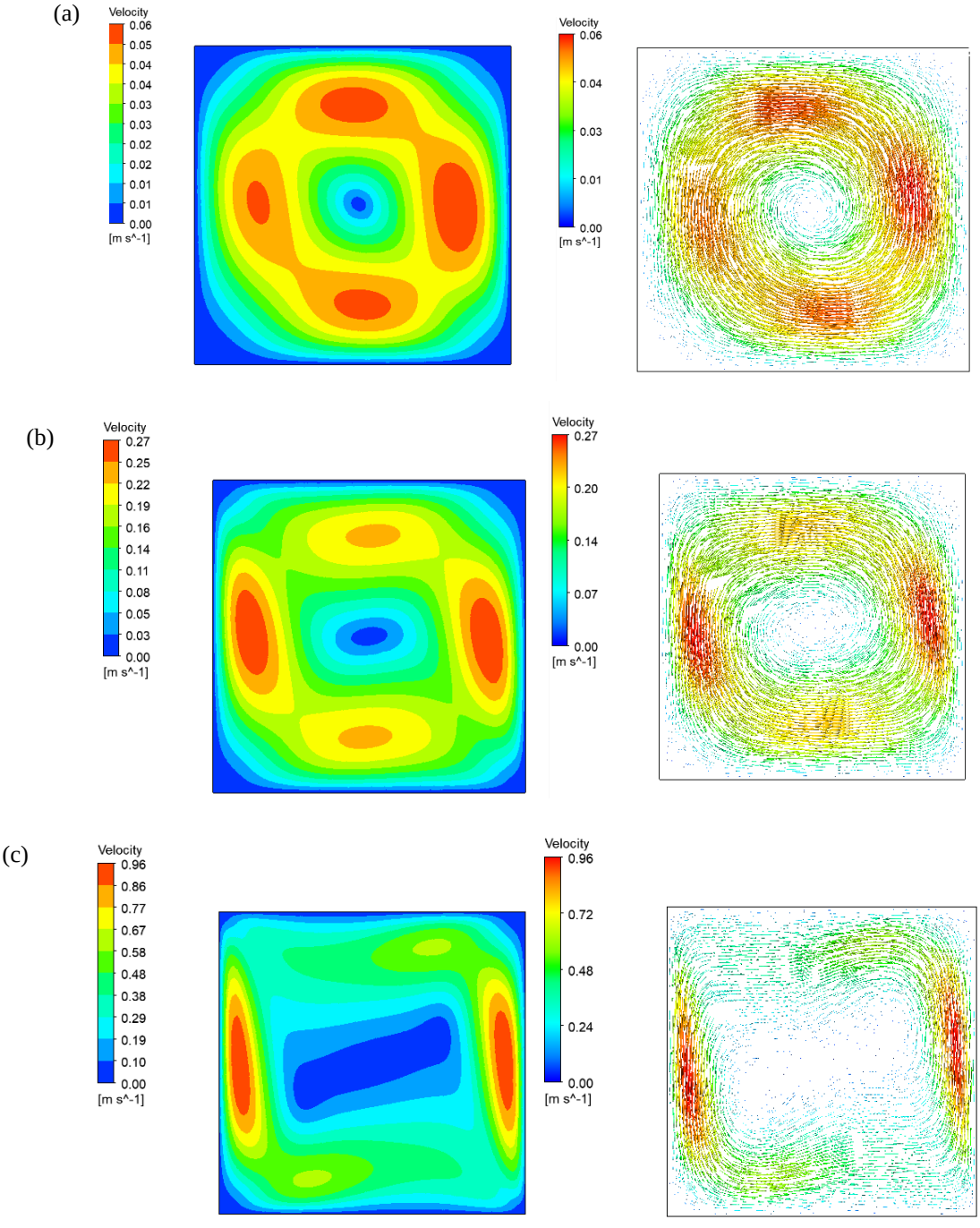

Figure 2 Velocity contour and vector results for (a) Ra = 10^3, (b) Ra = 10^4, and (c) Ra = 10^5.

Stagnant zone from inside of the cavity can be seen to all three Rayleigh number case results. As the Rayleigh number increases, the stagnant zone started to widen until velocities are more focus to the active wall temperatures rather than adiabatic side of the walls. According from Kane, Mbow, Sow, and Sarr (2017), the existence of the stagnant zone indicates of heat transfer taking place in an intense way located at the corners of

the square cavity and at high Rayleigh number the circulation flow is more set to the upper left side and to lower right side forming a symmetrical flow of two cells recirculation filling the cavity. However, Kane, Mbow, Sow, and Sarr (2017) study [62-69] was conducted by having partially active walls, while this report focuses on full side of active walls. The recirculation did not focus on the upper corner left side and lower corner right side of the walls.

High Rayleigh number from 10^5 the recirculation was more focus to the active thermal side of the cavity wall. As the flow circulate in the cavity due to the temperature differences of the cavity walls, each different Rayleigh number case effects the fluid motion differently. The flow circulates in anticlockwise direction forming a vertex surrounds the stagnant zone. Based from the results of velocity contour that as the Rayleigh number increases so does the buoyancy forces and convection inside the cavity causing the flow for convection of air increase intensely. At the heated region of the wall, the air was less dense and transport upward due to the buoyancy force. At cold region of the wall, flow was transport downward. Since top and bottom side of the walls were adiabatic, fluid flows inside the cavity with no heat transfer or changes. The circulation surrounding the cavity walls can be seen when the Rayleigh number is at 10^3 and 10^4. When the Rayleigh number at 10^5 from figure 2 that the flow was more focus to the active walls and less to the adiabatic walls. The recirculation was due to the flow when leaving the hot or cold region of the wall, the air was freely move to upward or downward direction. This recirculation indicates symmetrical flow of a fluid.

Validation was taken by comparing the present numerical results of average Nusselt number from Ansys Fluent software with previous researchers that have conducted studies relating to the natural convection inside square cavity. Table below are the presented result taken from Ansys and compare with previous studies.

Table 2 Nusselt number from Ansys Fluent compared to previous studies.

Rayleigh number	Nusselt number (de Vahl Davis, 1983)	Nusselt number (Nithiarasu et al., 1997)	Nusselt number (A.Raisi, 2018)	Present
10^3	1.116	1.127	1.118	1.117
10^4	2.238	2.245	2.246	2.248
10^5	4.509	4.521	4.523	4.531

The experimental results provide similarly to those studies natural convection from previous researchers and how different Rayleigh number can affect the fluid flow inside the cavity. Such as at low Rayleigh number flow of fluid filled the cavity and when the Rayleigh number increases, the recirculation appeared and was more focus on to the active thermal sides of the walls. Stagnant zone appeared to all three Rayleigh number cases that indicated of heat transfer located at the center cavity. Because the results taken from Ansys fluent were similar from previous studies, it can be concluded that Ansys fluent can also be used for CFD solver and heat transfer modelling.

IV. PROPOSED WORK FOR CABLE TUNNEL CASE

After investigated the benchmark case, a 3D tunnel model was constructed with simplified by having only the right compartment of half a tunnel. The approach from simplified was to be made it easier to replicate of an actual model to be use for analysis and easy processing to provide valid results. Front side of the tunnel is where the inlet for air to flow until to the outlet of the tunnel. Thickness of the wall were carried out by the Ansys Fluent for the conduction effect and assumed with no-slip wall condition. For this study two tunnel models were constructed with the use of Design Modeler from Ansys Fluent. The two tunnel models have a different number of cable troughs of one cable trough and three cable troughs with the tunnel length having 100 m. The tunnel models have two different kind of cable circuits with the first cable circuit located on the bottom of the tunnel and surround with concrete. As for the other cable circuits is the cable trough, an air-filled housing for cables that attached on the side of the inner tunnel. Both cable circuits have water pipes installed with copper cables. Figure 3 is how the cable circuits are arranged in the tunnel.

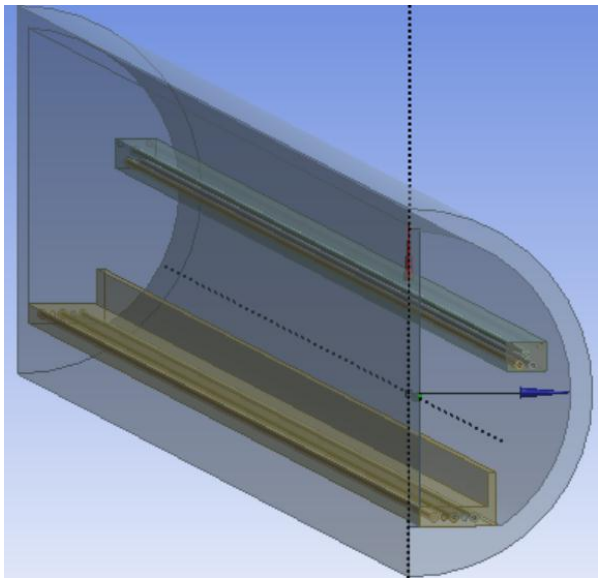

Figure 3 On the side of the tunnel is the cable trough and the one on the bottom is the cable circuit surround with concrete.

This study was to compare the heat efficiency based from the number of cable troughs and determine which was more efficient based with given different water flow rates and heat loads scenarios. Due to the copper cable generated large amount of heat inside the cable trough, water pipes and air inside the troughs were used to remove the heat to prevent overheating. As the heat was removed from the cable trough, it was transferred by the air from the tunnel's air ventilation to the tunnel outlet. During the heat transfer by air, some of the heat was conducted through the tunnel concrete walls and causing the heat transferred into the ground soil. Figure 4 shows how the tunnel model design with different number of cable troughs.

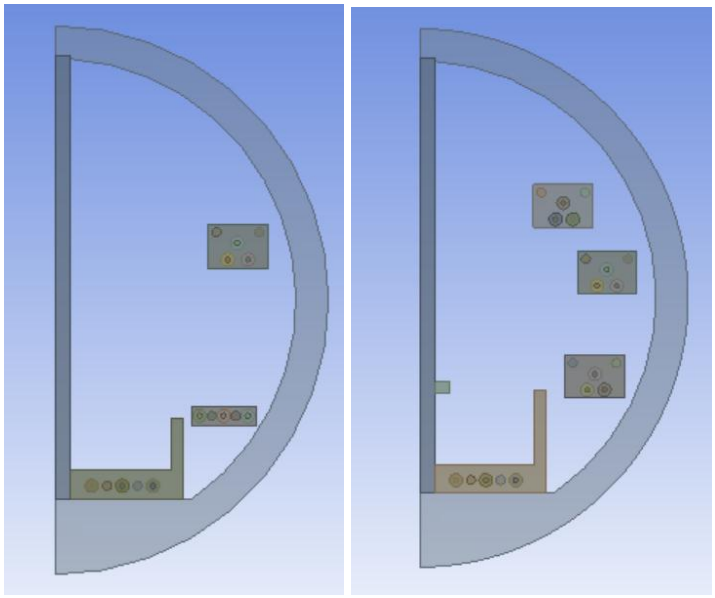

Figure 4 Comparison view for tunnel with one cable trough and three cable troughs.

For tunnel with one cable trough has two bottom cable circuit based on the design from Singapore cable tunnel and for the design of the three cable troughs was by replacing one of the bottom circuits with another cable trough. As for the water pipes from the cable circuits were in counterflow direction. This due to counterflow direction provide more maximum efficiency of heat transfer. Figure 5 shows how the direction of the water pipes.

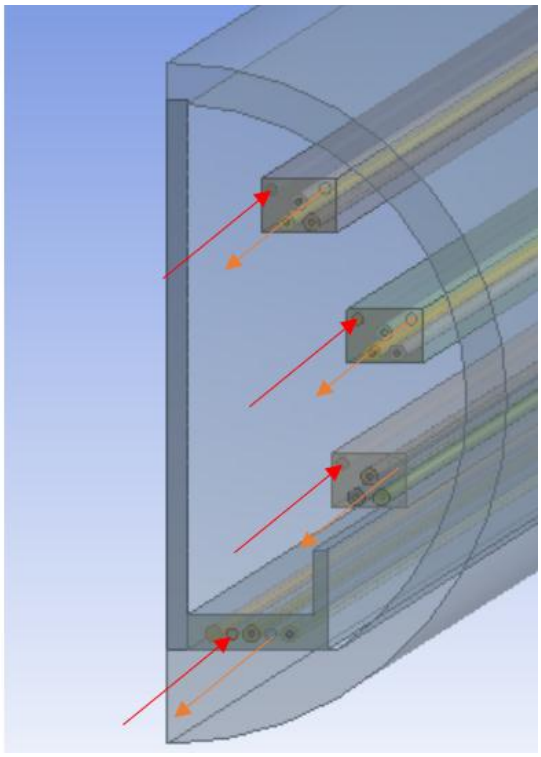

Figure 5 Water flow direction from the water pipes.

The red arrow indicated inlet flow of the water flowrates and orange arrow for outlet water flow, both directions causing a counterflow heat exchanger with the cables. Different scenarios for the tunnel model were based on heat loads and water flowrate for each model. The energy source for each scenarios case were set at different values based on the heat loads scenarios. The heat source value use for bottom concrete was 120 W/m per circuit and the air-filled cable trough has the heat dissipation rate of 113 W/m per circuit. Based on the heat release for number of cable trough and existing cable circuits in the tunnel, the heat dissipation for one cable trough tunnel model was 30 W/m per cable, while the three troughs model was 40 W/m per cable. Table 3 present how different scenarios were implemented for the two tunnel models.

Table 3 List of scenarios cases.

Case No.	Number of cable troughs	Heat load %	Water flowrate
1	1	100%	4.25 L/s
2	1	100%	6.5 L/s
3	1	70%	4.25 L/s
4	1	70%	6.5 L/s
5	3	100%	4.25 L/s
6	3	100%	6.5 L/s
7	3	70%	4.25 L/s
8	3	70%	6.5 L/s

The tunnel model has the radiation exchange in an enclosure of gray-diffuse surfaces. The exchange of energy between two different surfaces depends on the size, distance, and orientation based on Surface to Surface (S2S) Radiation Model Theory. The model neglects any absorption, emission, or scatter of radiation. As it focuses on surface-to-surface radiation. The advantages of this model provide good modelling transfer of radiative without the need for participating media. Limitation of this model is unable to be used for participating radiation problems, does not support semi-transparent boundaries, and does not support hanging nodes or hanging node adaption on radiating boundary zones. The S2S model equations are based on the energy flux transfer from a surface with emitted and reflected energy. Energy leaving from a surface is based on a reflected energy flux relying on the incident energy flux from the surroundings. As discussed from the benchmark case, fluid is heated, the density of the fluid varies with temperature and flow of the fluid can be affected by force of gravity based on the density variation. The buoyancy force in a natural convection flow can be measured with the ratio of dimensionless number Grashof number and Reynolds numbers.

Standard k-ε model was used for this case. The standard k-ε model is one of two equation model that determine the turbulent length and time scale through the two transport equations. The transport equations are based from kinetic energy (k) of the turbulence and the dissipation rate (ε). For this standard model of a turbulence, the assumption made is that it is fully turbulence and the effects of molecular viscosity are negligible. The standard k-ε model transport equation can be shown below.

$$\frac{\partial}{\partial t}(\rho k) + \frac{\partial}{\partial x_i}(\rho k u_i) = \frac{\partial}{\partial x_j}\left[\left(\mu + \frac{\mu_t}{\sigma_k}\right)\frac{\partial k}{\partial x_j}\right] + G_k + G_b - \rho\varepsilon - Y_m + S_k \quad (1)$$

$$\frac{\partial}{\partial t}(\rho \varepsilon) + \frac{\partial}{\partial x_i}(\rho \varepsilon u_i) = \frac{\partial}{\partial X_j}\left[\left(\mu + \frac{\mu_t}{\sigma_\varepsilon}\right)\frac{\partial \varepsilon}{\partial x_j}\right] + C_{1\varepsilon}\frac{\varepsilon}{k}\left(G_k + G_{3\varepsilon}G_b\right) - G_{2\varepsilon}\rho\frac{\varepsilon^2}{k} + S_\varepsilon \quad (2)$$

G_k is the kinetic energy of turbulence due from the mean velocity gradients, and G_b is the kinetic energy of turbulence due to the buoyancy force. Y_m is the contribution of the fluctuating dilatation in compressible turbulence to the overall dissipation rate. $C_{1\varepsilon}$, $C_{2\varepsilon}$, and $C_{3\varepsilon}$ are constants. $\sigma_{k \text{ and}}\ \sigma_\varepsilon$ are the turbulent Prandtl number for the kinetic energy and dissipation rate. S_k and S_ε are terms for user-defined sources.

Based on the system, the energy balance can depend on the surroundings. It can be isolated, open system, and closed system. Isolates are where there is no energy or mass transfer between the system and surroundings. The closed system has energy but no mass transfer while the open system has energy and mass transfer. For heat it uses Q represents the energy flow due to the temperature difference can usually be defined as positive when transferred from surroundings to the system. To analyze the heat transfer rate from cable tunnel system by air, water, and ground the heat balance in a system as heat generated by copper in the cable can be arranged for the equation shown below.

$$Q_{total} = Q_{water} + Q_{ground} + Q_{air} \quad (3)$$

To determine the heat energy of water and air, it can be determined by general heat energy equation by multiplication of mass (M), specific heat (C), and change of temperature (ΔT). The equations for water and air can be rewritten below.

$$Q_{water} = C_{water}M_{water}(T_{out} - T_{in}) \quad (4)$$

$$Q_{air} = C_{air}M_{air}(T_{out} - T_{in}) \quad (5)$$

For ground is based on the heat transfer coefficient multiple by the different temperatures from the tunnel wall and temperature ambient.

$$Q_{ground} = heat\ transfer\ coefficient\ \times (T_{tunnelwall} - T_{ambient}) \quad (6)$$

Q_{total} can be represented as heat generated by the copper wire from the cable tunnel system which the equation can be written as.

$$Q_{total} = L \times q \times n \quad (7)$$

L is the length of the copper core, q is the cable circuit heat generation rate, and n is the number of cable circuits.

Temperature contours and vector results are illustrated based from the eight different case scenarios with different numbers of cable troughs for 100% and 70% heat load and as well with water mass flow rate of 4.25 L/s and 6.5 L/s. Results were taken at XY plane of the geometry model at central tunnel of 50 m. For some cable troughs the heat transfer was expected to be higher than the rest of the cable circuit. The reason for low heat transfer from some of the cable troughs could due to some only have the natural convection occur while the other cable circuits have exchange heat through conductivity. Figure 6 and Figure 7 shows the temperature contour for one cable trough and as for three cable troughs at Figure 8 and Figure 9.

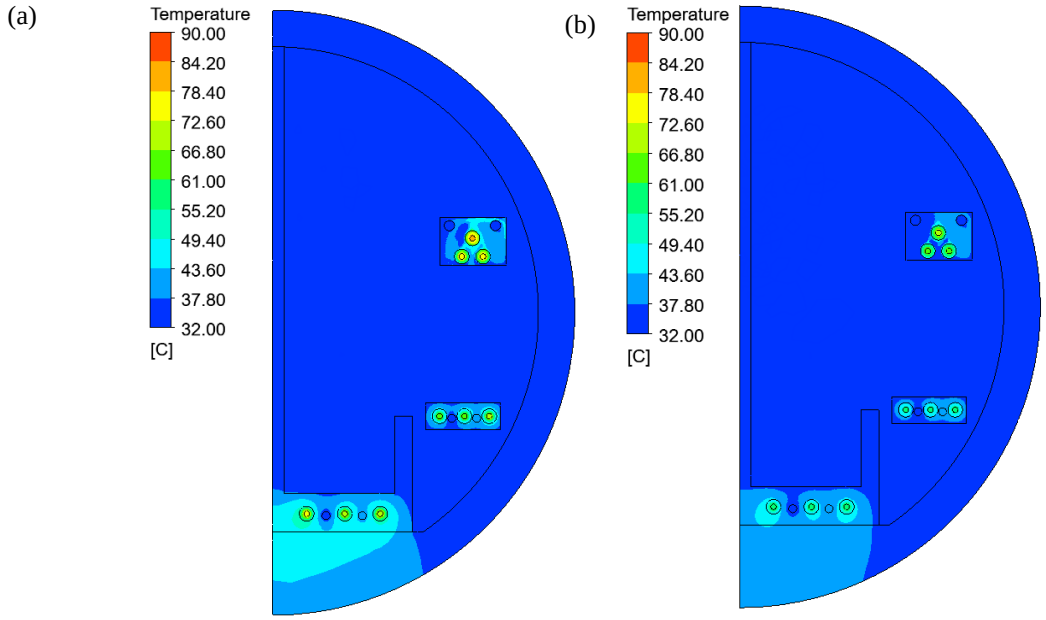

Figure 6 Tunnel with one cable trough temperature contour results for (a) 100% heat load and (b) 70% heat load with 4.25 L/s water flow rate.

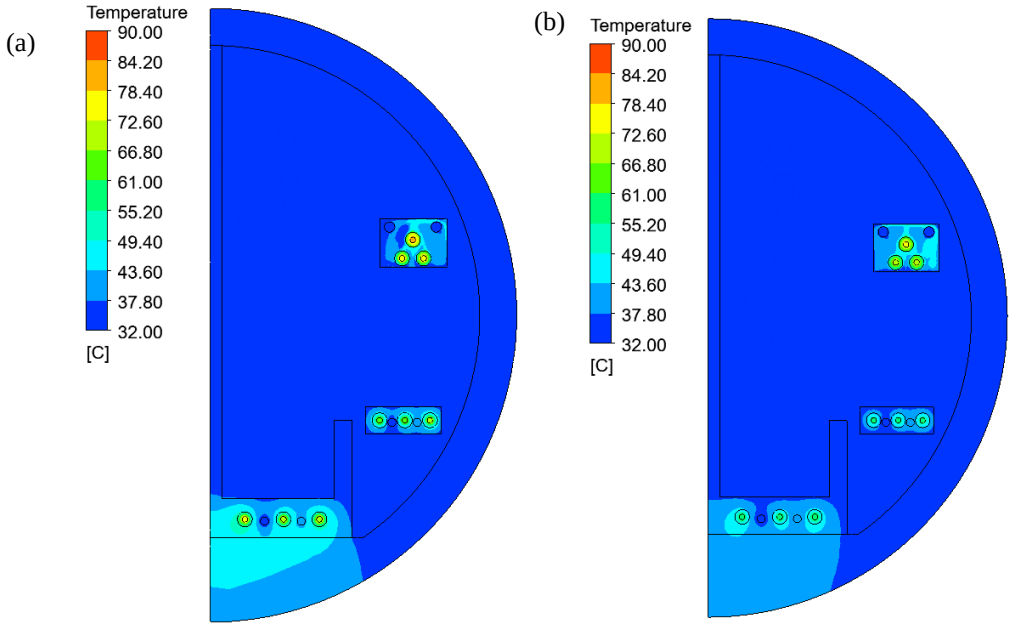

Figure 7 Tunnel with one cable trough temperature contour results for (a) 100% heat load and (b) 70% heat load with 6.5 L/s water flow rate.

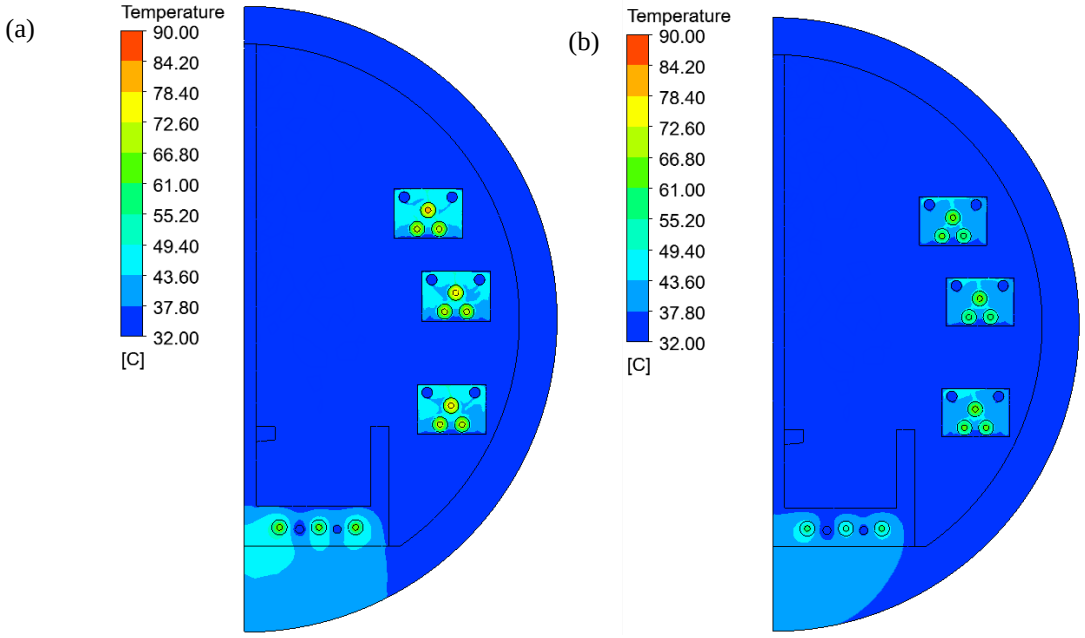

Figure 8 Tunnel with three cable troughs temperature contour results for (a) 100% heat load and (b) 70% heat load with 4.25 L/s water flow rate.

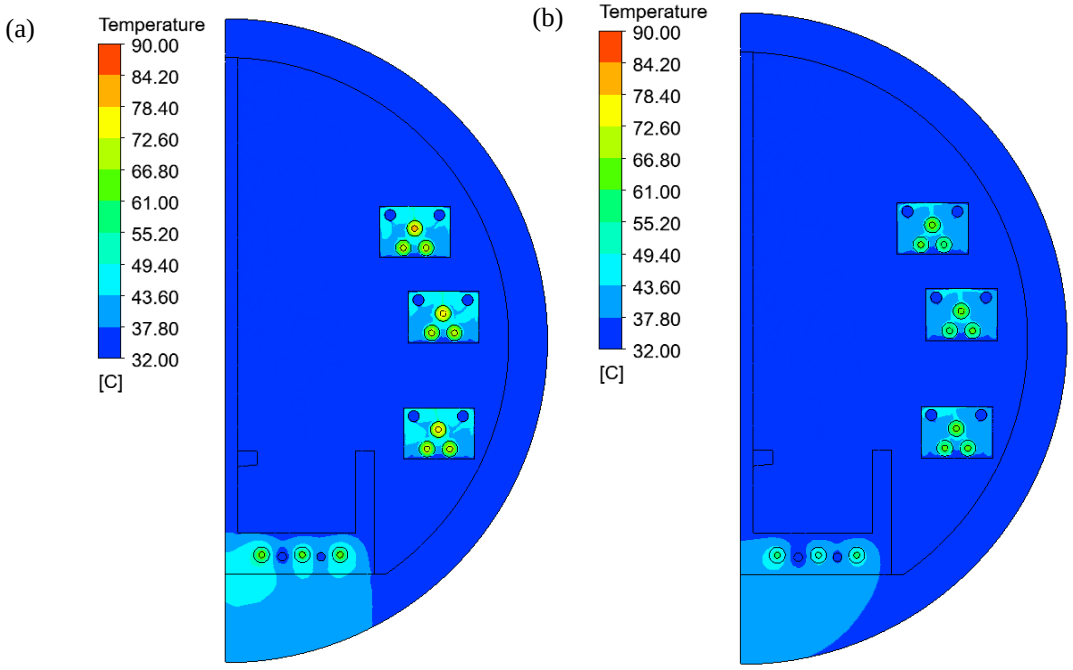

Figure 9 Tunnel with three cable troughs temperature contour results for (a) 100% heat load and (b) 70% heat load with 6.5 L/s water flow rate.

Temperature contours for one cable trough result for heat load 100% from figure 6 show the air surrounding inside the cable trough experience differently on how air removes heat from copper cable. For heat load 100% and 70% with water mass flow rate of 6.5 L/s having higher air temperature, this could be due to faster flow rate from the water pipes in counterflow direction increases heat transfer resulting air taken away more heat by sending the removed heat to outside of the cable circuit. For bottom circuits of the tunnel, heat from both circuits were mostly removed by conductivity heat transfer to the wall tunnel which continue to the ground soil. For the three cable troughs model similarly with the results from tunnel one cable trough, a larger flow rate provides a better heat transfer but with additional number of cable trough the heat transfer for different heat loads

and water flow rates were similar. Inside the cable trough, the airflow experiences a recirculation during the heat transfer of natural convection similarly from the benchmark case that can be shown at figure below.

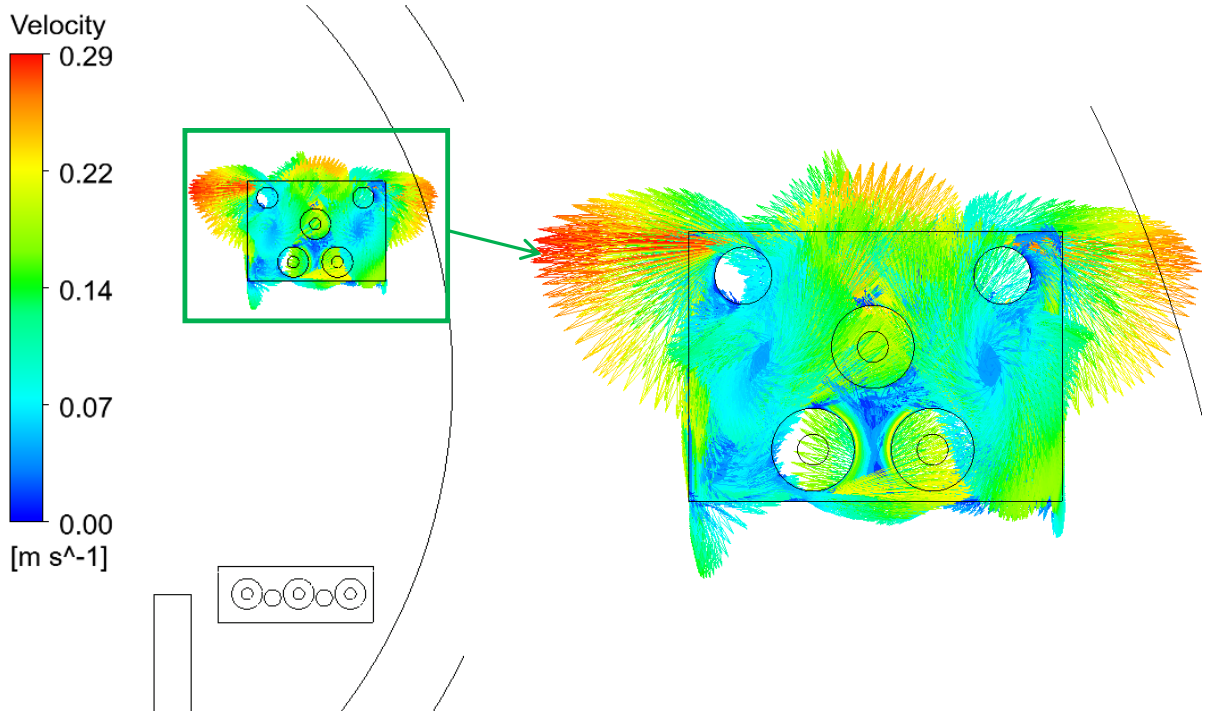

Figure 10 Enlarge view for natural convection inside the cable trough for heat load 100% with water flow rate 4.25 L/s.

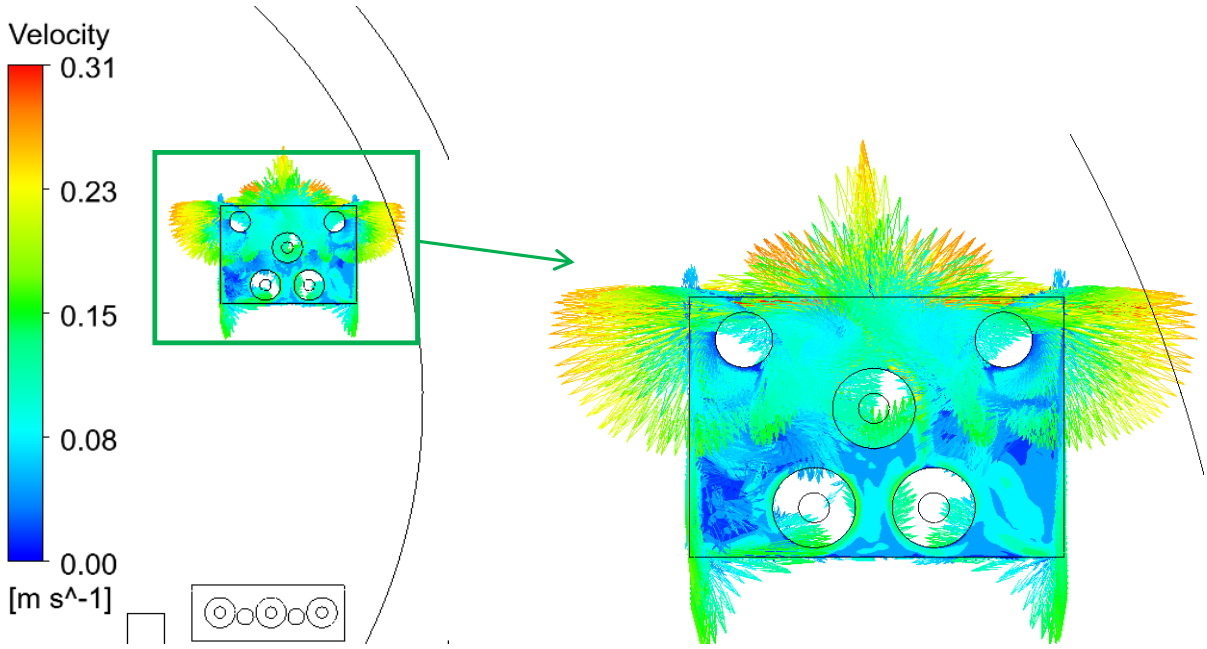

Figure 11 Enlarge view for natural convection inside the cable trough for heat load 100% with water flow rate 6.5 L/s.

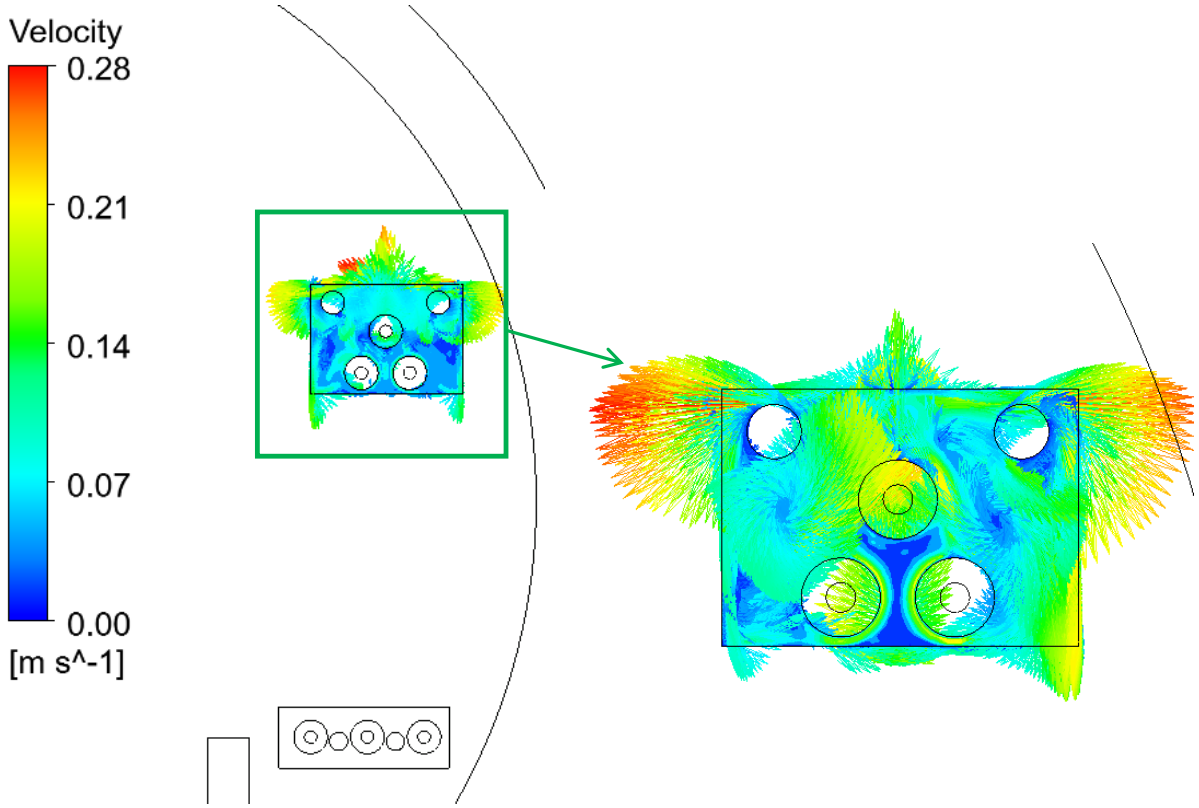

Figure 12 Enlarge view for natural convection inside the cable trough for heat load 70% with water flow rate 4.25 L/s.

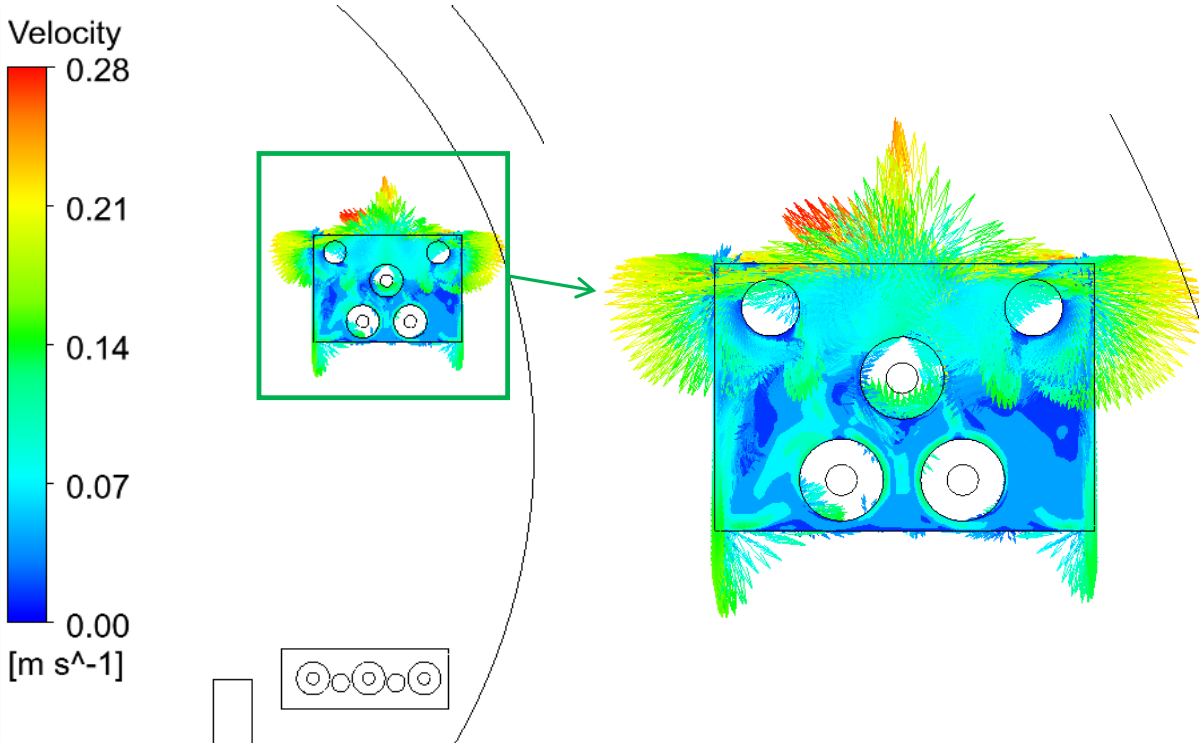

Figure 13 Enlarge view for natural convection inside the cable trough for heat load 70% with water flow rate 6.5 L/s.

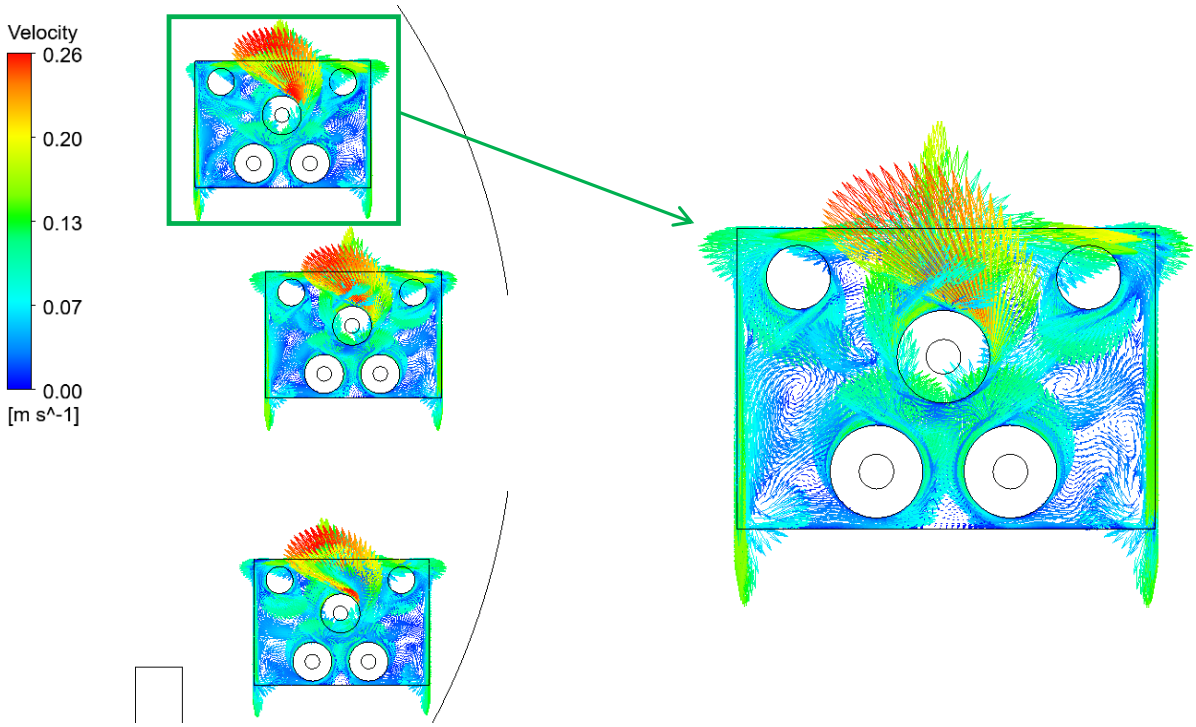

Figure 14 Enlarge view for three cable troughs for heat load 100% with water flow rate 4.25 L/s.

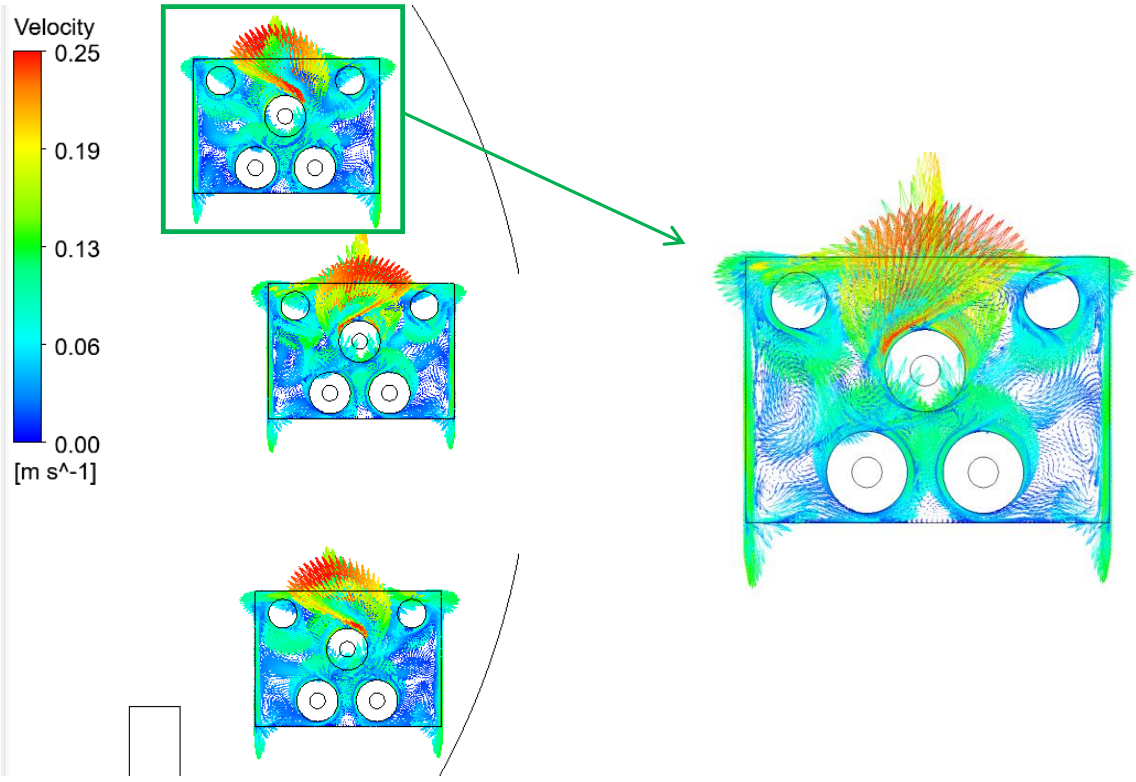

Figure 15 Enlarge view for three cable troughs for heat load 100% with water flow rate 6.5 L/s.

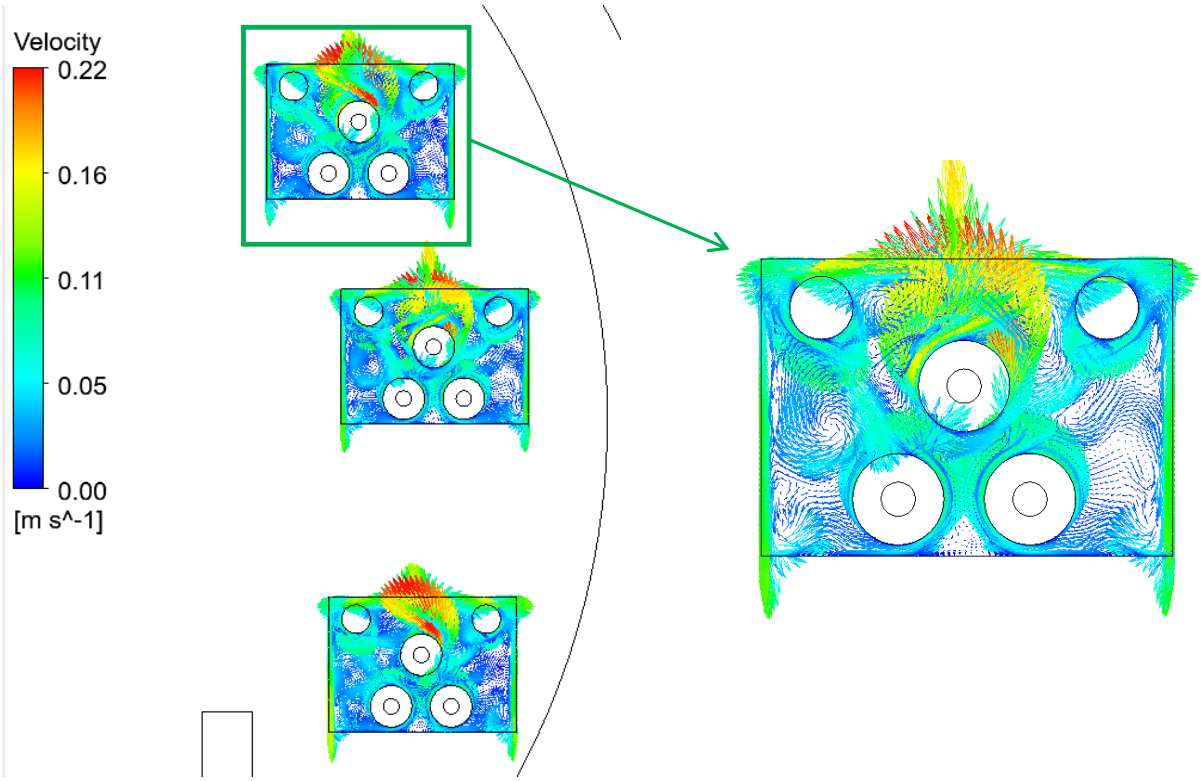

Figure 16 Enlarge view for three cable troughs for heat load 70% with water flow rate 4.25 L/s.

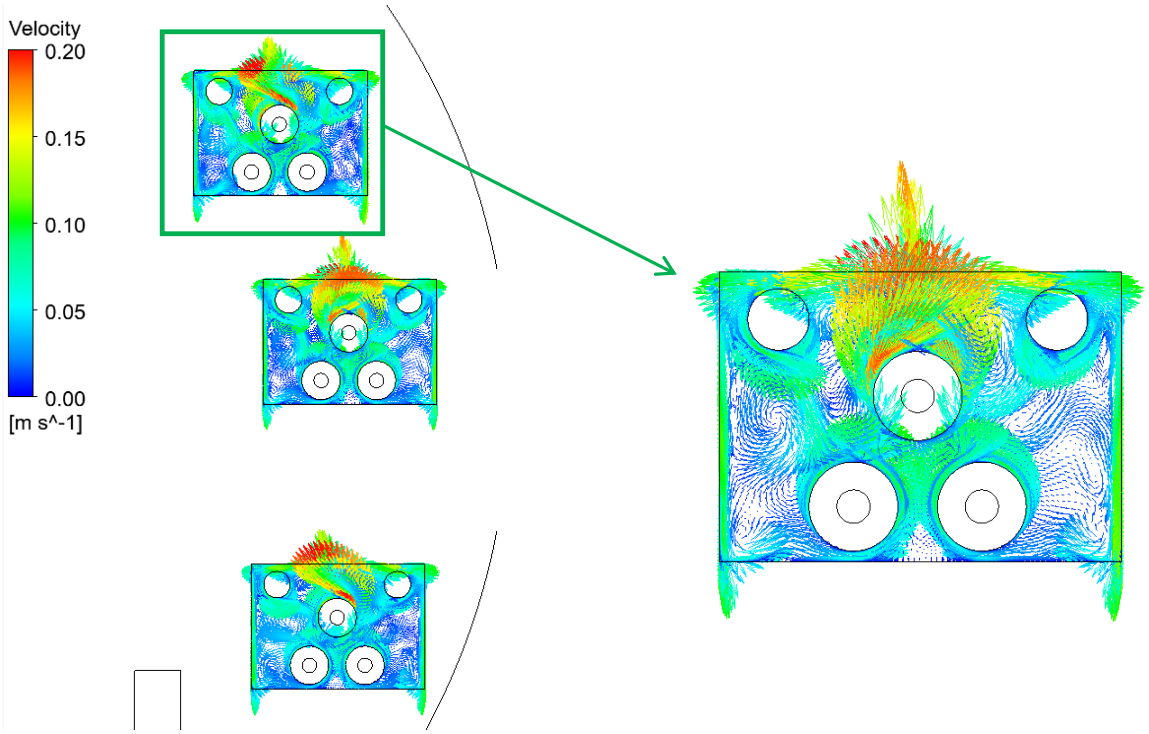

Figure 17 Enlarge view for three cable troughs for heat load 70% with water flow rate 6.5 L/s.

The aerodynamic inside the cable trough circuit for tunnel model with one cable trough can be seen in Figure 10, Figure 11, Figure 12, and Figure 13 for enlarged view velocity vector on how air rise due to high temperature and go down when air cool down. A circulation present at different areas of the cable trough circuit

due to direction movement of air at different temperature. Based from benchmark case natural convection inside the square cavity that a circulation is present through natural convection by buoyancy force. As for cable tunnel with three cable troughs behave differently than tunnel with one cable trough, the circulation was mostly located on the top center spot from the top three cable trough circuit and less to near the water pipes.

From Ansys Fluent, temperature changes were recorded for temperature outlet of water, air, and the conductivity to the ground. Heat relocation results were calculated for 100-meter tunnel model are presented below with two tables based on the one cable trough model and three cable troughs model respectively.

Table 4 Summary of CFD results for tunnel with three cable troughs.

Component	100% Heat load with 4.25 L/s	100% Heat load with 6.5 L/s	70% Heat load with 4.25 L/s	70% Heat load with 6.5 L/s	Criteria
Tunnel Air (℃)	32.0 → 32.61	32.0 → 32.62	32.0 → 32.44	32.0 → 32.44	≤ 45 ℃
Water pipe within cable trough filled air, Top (℃)	32.0 → 32.10	32.0 → 32.04	32.0 → 32.07	32.0 → 32.03	≤ 45 ℃
Water pipe within cable trough filled air, middle (℃)	32.0 → 32.10	32.0 → 32.04	32.0 → 32.07	32.0 → 32.03	≤ 45 ℃
Water pipe within cable trough filled air, bottom (℃)	32.0 → 32.11	32.0 → 32.04	32.0 → 32.08	32.0 → 32.03	≤ 45 ℃
Water pipe within bottom cable circuit (℃)	32.0 → 32.22	32.0 → 32.09	32.0 → 32.15	32.0 → 32.06	≤ 45 ℃
Maximum copper (℃)	74.10	78.76	66.18	66.36	< 90 ℃
Water flow rate in pipe of cable trough Air filled at top (L/s)	4.25	6.5	4.25	6.5	-
Water flow rate in pipe of cable trough Air filled at middle (L/s)	4.25	6.5	4.25	6.5	-
Water flow rate in pipe of cable trough Air filled at bottom (L/s)	4.25	6.5	4.25	6.5	-
Water flow rate in pipe of bottom circuit (L/s)	4.25	6.5	4.25	6.5	-
Total water flow rate (L/s)	12.75	19.5	12.75	19.5	-
Maximum air velocity (m/s)	3.22	3.23	3.23	3.22	≤ 5 m/s
Average Air velocity (m/s)	2.73	2.73	2.73	2.73	-
Heat transfer Water	20.52%	12.44%	15.11%	8.89%	-
Heat transfer Air tunnel	48.13%	48.52%	34.72%	34.72%	≤ 50%
Heat transfer Ground	31.35%	38.64%	50.96%	56.40%	-

Table 5 Summary of CFD results for tunnel with one cable trough.

Component	100% Heat load with 4.25 L/s	100% Heat load with 6.5 L/s	70% Heat load with 4.25 L/s	70% Heat load with 6.5 L/s	Criteria
Tunnel Air (℃)	32.0 → 32.59	32.0 → 32.65	32.0 → 32.44	32.0 → 32.47	≤ 45 ℃
Water pipe within cable trough filled air, bottom (℃)	32.0 → 32.08	32.0 → 32.04	32.0 → 32.06	32.0 → 32.03	≤ 45 ℃
Water pipe within bottom cable circuit (℃)	32.0 → 32.30	32.0 → 32.12	32.0 → 32.21	32.0 → 32.09	≤ 45 ℃
Water pipe within second circuit (℃)	32.0 → 32.25	32.0 → 32.10	32.0 → 32.17	32.0 → 32.07	≤ 45 ℃

Maximum copper (℃)	83.18	88.99	68.23	74.13	< 90 ℃
Water flow rate in pipe of cable trough Air filled (L/s)	4.25	6.5	4.25	6.5	-
Water flow rate in pipe of bottom cable circuit	4.25	6.5	4.25	6.5	-
Water flow rate in pipe of second cable circuit	4.25	6.5	4.25	6.5	-
Total water flow rate (L/s)	12.75	19.5	12.75	19.5	-
Maximum air velocity (m/s)	3.21	3.21	3.21	3.21	≤ 5 m/s
Average Air velocity (m/s)	2.73	2.73	2.73	2.73	-
Heat transfer Water	31.02%	20.02%	18.12%	14.63%	-
Heat transfer Air tunnel	60.53%	66.69%	45.14%	48.22%	≤ 50%
Heat transfer Ground	8.45%	13.29%	36.74%	37.15%	-

Conductivity to the ground from one cable trough model for 70% heat load and all three cable troughs result removed heat about 31% - 56%, which was very high for ground. The reasonable amount for ground should be around 10%. Majority of the heat should have taken out by water about 50% and the rest by air as it should be sending out through the outlet of the tunnel. Tunnel with three number of cable troughs for 100% heat load with water flow rate of 4.25 L/s is recommended for cooling efficiency, it provided heat release more efficiently and balance as it releases more by water 20.52% and air 48.13%. For air should not be higher than 50%, consideration for human being comfort inside the tunnel it was not recommended for air to be anything higher than 50%. For copper cable, the middle cable trough circuit from three cable troughs model has the highest temperature of 78.76 ℃ for 100% heat load, while for 70% heat load was 66.18 ℃. As for the one cable trough model reached temperature of 88.99 ℃ for 100% heat load and 74.13 ℃ for 70% heat load.

V. CONCLUSION

A 3D Computational Fluid Dynamics (CFD) analysis was conducted on a 100-meter cable tunnel system based on different number of cable troughs were investigated with eight scenarios cases. The scenario cases were based on varying cable circuit for heat load at 100% and 70%, with corresponding water flow rate of 4.25 L/s and 6.5 L/s. Just as the 2D square from benchmark case, the tunnels were modelled with no-slip wall boundary condition. The tunnel was design by only with a half tunnel of the right compartment side. This is meant to simplify the model as the approach from simplified was to be made it easier to replicate of an actual model to be use for analysis and easy processing to provide valid results. Each cable circuit housed two water pipes and three copper cables. As for the cable trough it was air-filled. The analysis focused on evaluating cooling efficiency by assessing heat loss through air and water. Heat from copper cables was transferred by the water flow in a counterflow direction, and the subsequent heat was expelled by air to outside of the tunnel. Results indicated that 100% heat load yielded higher temperature results than 70% heat load.

To choose which was providing less heat for a tunnel, the 70% heat load met the criteria as it was sufficient for generating less heat. For criteria given of max temperature for copper cables must be less than 90 ℃, both heat load scenarios passed the criteria. Copper cable from the three cable troughs model produced less heat than from one cable trough model. The heat relocation for one trough model shown for 100% heat load with 6.5 L/s had heat removed by air 66.69% and conductivity to the ground about 13.29%. As for 100% heat load with 4.25 L/s the conductivity ground was 8.45% with heat removed by air 60.53%. The more reasonable amount for ground should be around 10%. Results for one cable trough model at 70% heat load for all water flow rate scenarios and results for all three cable troughs scenarios, the heat transfer to the ground was high from 30-56%, resulting in insufficient heat relocation by air and water.

To determine the better choice of cooling efficiency was by which scenario has more balance with heat relocation by water and reasonable amount for air despite the high conductivity to the ground. Conclusion for the simulations, the tunnel model with three cable trough model provided a better choice compared tunnel with one cable trough. The one cable trough model heat relocation met the cooling requirements criteria for water and ground, but due to the air was heated up too much for about 66.69%, not recommended for human to be inside the tunnel. It is to be noted that Ansys Fluent Student and Teaching version were used to run these simulations, for an actual tunnel model design it is recommended require a much more powerful PC specifications for RAM and better CPU or GPU. It also suggested for Industry version for Ansys to be used for better accurate result. For a model to close as an industrial version, it is suggested the length of tunnel should be around 2000-3000 meters.

REFERENCES

[1] Convective Heat Transfer (2003). Retrieved from The Engineering Toolbox: https://www.engineeringtoolbox.com/convective-heat-transfer-d_430.html

[2] Davies, G., Revesz, A., & Maidment, G. (2019). Electrical cable tunnel cooling combined with heat recovery, in cities. London: The School of Engineering, London South Bank University.

[3] Jensen, O., & Adi-Zadeh, D. (1988). Heat transfer and thermal stresses in the Singapore cable tunnel. ABSE congress report = Rapport du congrès AIPC = IVBH.

[4] Kai, Y., Xiaodong, Z., Lizhong, Y., Xiao, T., Yuan, Z., Bei, C., . . . Yong, N. (2019). A Multi-Scale Analysis of the Fire Problems in an Urban Utility Tunnel. Energies.

[5] Kane, M. K., Mbow, C., Sow, M. L., & Sarr, J. (2017). A Study on Natural Convection of Air in a Square Cavity with Partially Thermally Active Side Walls.

[6] Natural Convection in Square Cavity. (n.d.). Retrieved from FEATool Multiphysics: https://www.featool.com/model-showcase/06_Multiphysics_04_natural_convection1/

[7] Raisi, A., & Arvin, I. (2018). A numerical study of the effect of fluid-structure interaction on transient natural convection in an air-filled square cavity. Internasional Journal of Thermal Sciences, 1-14.

[8] Surface to Surface (S2S) Radiation Model Theory. (n.d.). Retrieved from Ansys: https://www.afs.enea.it/project/neptunius/docs/fluent/html/th/node116.htm

[9] T. Bragatto, M. C. (2019). A 3-D nonlinear thermal circuit model of underground MV power cables and their joints. ELectric Power Systems Research, 112-121.

[10] Yunzhang, Z., & Yanren, H. (2014). The Crank-Nicolson Extrapolation Stabilized Finite
Ansys. (n.d.). Ansys Help. Retrieved from Ansys: https://ansyshelp.ansys.com/

[11] Surface to Surface (S2S) Radiation Model Theory. (n.d.). Retrieved from Ansys: https://www.afs.enea.it/project/neptunius/docs/fluent/html/th/node116.htm

[12] Simulation Example - Natural Convection in a Square Cavity. (n.d.). Retrieved from Ansys: https://courses.ansys.com/index.php/courses/what-are-fluids/lessons/simulation-examples-homework-and-quizzes/topic/simulation-example-natural-convection-in-a-square-cavity/

[13] Yunzhang, Z., & Yanren, H. (2014). The Crank-Nicolson Extrapolation Stabilized Finite Element. Hindawi Publishing Corporation.

[14] Geoengineer.org. (2017, December 20). geoengineer.org. Retrieved from geoengineer: https://www.geoengineer.org/news/singapore-deepest-transmission-cable-tunnel-system-ready Bahrami, M. (n.d.). Natural Convection. SFU, 1-7.

[15]. Parker, C. M. (2016). The effect of tip speed ratio on a vertical axis wind turbine at high Reynolds numbers. Springer Link, 74.

[16]. Ross, P. J. (1996). Taguchi techniques for quality engineering : loss function, . New York: McGraw-Hill.

[17]. Singapore: A leading Manufacturing hub. (2018, May 21). Retrieved from EDB Singapore: https://www.edb.gov.sg/en/business-insights/insights/singapore-a-leading-manufacturing-hub.html

[18]. Smith, A. (2015). George Edward Pelham Box. London: Royal Society.

[19]. Songwang. (2023, Auguest 10). Randomized Complete Block Design with and Without Subsamples. Retrieved from Pages.stat.wisc.edu: https://pages.stat.wisc.edu/~songwang/RCBD.pdf

[20]. ST&D. (2023, November 25). Topic 6. Randomised Complete Design (RCBD). Retrieved from Psfaulty.plantsciences: https://psfaculty.plantsciences.ucdavis.edu/agr205/Lectures/2011_Lectures/L6_RCBD.pdf

[21]. UK, N. U. (2023, Novmber 29th). Numercy, Maths, and Statistics - Academic Skill Kit. Retrieved from ncl.ac.uk: https://www.ncl.ac.uk/webtemplate/ask-assets/external/maths-resources/statistics/regression-and-correlation/coefficient-of-determination-r-squared.html#:~:text=6%20See%20Also-,Definition,line%20approximates%20the%20actual%20data.

[22]. Kok, C.L.; Siek, L. Designing a Twin Frequency Control DC-DC Buck Converter Using Accurate Load Current Sensing Technique. Electronics 2024, 13, 45. doi: 10.3390/electronics13010045

[23]. R. K. Gupta and S. K. Arora, "Thermal Management of High-Capacity Cable Tunnels Using Enhanced Cooling Technologies," IEEE Transactions on Industry Applications, vol. 51, no. 4, pp. 3046-3053, July/August 2015.

[24]. M. S. Kumar and V. R. Reddy, "Optimization of Cable Tunnel Designs for Improved Heat Dissipation and Cooling," IEEE Transactions on Power Delivery, vol. 35, no. 1, pp. 712-719, February 2020.

[25]. Kok, C.L.; Chia, K.J.; Siek, L. A 87 dB SNR and THD+N 0.03% HiFi Grade Audio Preamplifier. Electronics 2024, 13, 118. doi: 10.3390/electronics13010118

[26]. C. M. Liao and T. K. Chou, "Thermal Analysis of Cable Tunnels Using a Numerical Method," IEEE Transactions on Power Delivery, vol. 11, no. 3, pp. 1496-1502, July 1996.

[27]. A. M. Gaudet and D. M. Taghavi, "A Study of Cable Tunnel Temperature Distribution and Cooling Requirements," IEEE Transactions on Industry Applications, vol. 31, no. 2, pp. 432-439, March/April 1995.

[28]. G. M. Zobrist and K. K. Wong, "Thermal Performance Analysis of Electrical Cable Systems in High-Density Cable Tunnels," IEEE Transactions on Power Delivery, vol. 16, no. 4, pp. 900-906, October 2001.

[29]. J. M. Rodríguez and F. M. González, "Optimization of Cooling Systems in Cable Tunnels for Enhanced Thermal Management," IEEE Transactions on Power Electronics, vol. 26, no. 5, pp. 1420-1427, May 2011.

[30]. Ullah, M. I. (2015, August 25). Randomized Complete Block Design. Retrieved from Basic Statistics and Data Analysis: https://it-feature.com/design-of-experiment-doe/randomized-complete-block-design

[31]. Young, L. S. (2020, March 19). Notation for the Population Model. Retrieved from STAT 501: https://online.stat.psu.edu/stat501/

[32]. Zach. (2020, November 6th). Statology. Retrieved from What is Stepwise Selection? (Explanation & Examples): https://www.statology.org/stepwise-selection/

[33]. H. K. Wong and W. S. Chan, "Evaluation of Cooling Strategies for High Heat Load Cable Tunnels," IEEE Transactions on Power Delivery, vol. 22, no. 4, pp. 2345-2352, October 2007.

[34]. K. R. Gopalakrishnan and S. R. Kannan, "Impact of Additional Cable Troughs on Cooling Efficiency in Cable Tunnels," IEEE Transactions on Power Delivery, vol. 29, no. 3, pp. 1140-1147, July 2014.

[35]. H. Y. Park and J. S. Lee, "Evaluation of Cable Tunnel Cooling Systems with Additional Cable Troughs," IEEE Transactions on Power Delivery, vol. 33, no. 5, pp. 2198-2206, October 2018.

[36]. F. L. Souza and J. M. Ribeiro, "Comparative Thermal Analysis of Cable Tunnels with Different Cooling Mechanisms," IEEE Transactions on Power Delivery, vol. 29, no. 6, pp. 2755-2762, December 2014.

[37]. Kok, C.L.; Tang, H.; Teo, T.H.; Koh, Y.Y. A DC-DC Converter with Switched-Capacitor Delay Deadtime Controller and Enhanced Unbalanced-Input Pair Zero-Current Detector to Boost Power Efficiency. Electronics 2024, 13, 1237. doi: 10.3390/electronics13071237

[38]. L. C. Yang and Y. Z. Lin, "Numerical Simulation of Cable Tunnel Cooling with Multiple Trough Configurations," IEEE Transactions on Industry Applications, vol. 48, no. 4, pp. 1250-1256, July/August 2012.

[39]. M. B. Guo and T. H. Chang, "Analysis of Cable Tunnel Cooling Performance with Various Cable Trough Configurations," IEEE Transactions on Power Delivery, vol. 27, no. 2, pp. 1135-1142, April 2012.

[40]. C. S. Lim and W. K. Choi, "Experimental Investigation of Cooling Efficiency in High-Density Cable Tunnels," IEEE Transactions on Power Electronics, vol. 31, no. 3, pp. 1589-1597, March 2016.

[41]. Zach. (2020, January 24th). Statology. Retrieved from A Simple Explanation of How to Interpret Variance: https://www.statology.org/a-simple-explanation-of-how-to-interpret-variance/

[42]. Teo, B.C.T.; Lim, W.C.; Venkadasamy, N.; Lim, X.Y.; Kok, C.L.; Siek, L. A CMOS Rectifier with a Wide Dynamic Range Using Switchable Self-Bias Polarity for a Radio Frequency Harvester. Electronics 2024, 13, 1953. doi: 10.3390/electronics13101953

[43]. J. P. Stuckey and K. L. Butler, "Impact of Ventilation and Heat Loads on Cable Tunnel Thermal Performance," IEEE Transactions on Industry Applications, vol. 49, no. 4, pp. 1643-1650, July/August 2013.

[44]. N. J. Patel and V. S. Singh, "Comparative Study of Cooling Mechanisms for High-Density Cable Tunnels," IEEE Transactions on Industry Applications, vol. 52, no. 1, pp. 43-50, January/February 2016.

[45]. S. T. Tan and M. C. Ho, "Thermal Management and Optimization for Cable Tunnels with Different Cable Trough Configurations," IEEE Transactions on Power Electronics, vol. 35, no. 5, pp. 5172-5180, May 2020.

[46]. G. R. Zhang and J. H. Zhang, "Numerical Modeling of Thermal Behavior in Cable Tunnels with Multiple Cable Circuits," IEEE Transactions on Industry Applications, vol. 55, no. 3, pp. 2356-2364, May/June 2019.

[47]. C. -L. Kok, Q. Huang, D. Zhu, L. Siek and W. M. Lim, "A fully digital green LDO regulator dedicated for biomedical implant using a power-aware binary switching technique," 2012 IEEE Asia Pacific Conference on Circuits and Systems, Kaohsiung, Taiwan, 2012, pp. 5-8, doi: 10.1109/APCCAS.2012.6418957.

[48]. H. H. Chen, M. L. Huang, and Y. F. Lai, "Thermal Analysis of Underground Cable Systems with Different Tunnel Configurations," IEEE Transactions on Power Delivery, vol. 25, no. 3, pp. 1352-1360, July 2010.

[49]. C. -L. Kok, X. Li, L. Siek, D. Zhu and J. J. Kong, "A switched capacitor deadtime controller for DC-DC buck converter," 2015 IEEE International Symposium on Circuits and Systems (ISCAS), Lisbon, Portugal, 2015, pp. 217-220, doi: 10.1109/ISCAS.2015.7168609.

[50]. L. Battisti, A. A. Castelli, and M. Benini, "Optimization of a Vertical Axis Wind Turbine using DoE technique," IEEE Transactions on Energy Conversion, vol. 24, no. 3, pp. 451-458, 2009.

[51]. P. C. Migliore, W. E. Johnson, and G. E. Waltz, "Design and analysis of a vertical-axis wind turbine," IEEE Transactions on Energy Conversion, vol. 22, no. 1, pp. 69-74, 2007.

[52]. A. S. Bahaj, L. Myers, and P. A. B. James, "Fundamentals applicable to the design of vertical axis wind turbines," IEEE Transactions on Energy Conversion, vol. 21, no. 3, pp. 549-555, 2006.

[53]. M. H. Mohamed, G. Janiga, E. Pap, and D. Thévenin, "Optimization of blade design for a vertical-axis wind turbine using simulated annealing," IEEE Transactions on Energy Conversion, vol. 25, no. 4, pp. 1037-1045, 2010.

[54]. C. Menet, "Design optimization of a vertical-axis wind turbine using Taguchi method and Response Surface Methodology," IEEE Transactions on Sustainable Energy, vol. 4, no. 2, pp. 293-302, 2013.

[55]. R. Howell, N. Qin, J. Edwards, and N. Durrani, "Wind tunnel and numerical study of a small vertical axis wind turbine," IEEE Transactions on Energy Conversion, vol. 26, no. 1, pp. 133-140, 2011.

[56]. W. Tjiu, T. Marnoto, M. Mat, M. Ruslan, and K. Sopian, "Optimization of vertical axis wind turbine performance using Taguchi method," IEEE Transactions on Sustainable Energy, vol. 6, no. 1, pp. 27-34, 2015.

[57]. B. S. P. R. Rao and M. J. V. Sundararajan, "Experimental investigation on the performance of a vertical axis wind turbine with variable aspect ratio," IEEE Transactions on Energy Conversion, vol. 29, no. 1, pp. 8-15, 2014.

[58]. A. S. Archer and M. Z. Jacobson, "Evaluation of global wind power," IEEE Transactions on Geoscience and Remote Sensing, vol. 51, no. 6, pp. 3435-3444, 2013.

[59]. F. Paraschivoiu, "Aerodynamic performance of H-Darrieus vertical axis wind turbines," IEEE Transactions on Energy Conversion, vol. 29, no. 1, pp. 8-15, 2012.

[60]. C. L. Kok, T. H. Teo, Y. Y. Koh, Y. Dai, B. K. Ang and J. P. Chai, "Development and Evaluation of an IoT-Driven Auto-Infusion System with Advanced Monitoring and Alarm Functionalities," 2024 IEEE International Symposium on Circuits and Systems (ISCAS), Singapore, Singapore, 2024, pp. 1-5, doi: 10.1109/ISCAS58744.2024.10558602.

[61]. D. K. Jain and S. K. Sharma, "Analysis of Heat Dissipation in Cable Tunnels: Effects of Varying Cable Troughs," IEEE Transactions on Power Delivery, vol. 30, no. 2, pp. 854-861, April 2015.

[62]. C. -L. Kok, L. Siek and W. M. Lim, "An ultra-fast 65nm capacitorless LDO regulator dedicated for sensory detection using a direct feedback dual self-reacting loop technique," 2012 IEEE International Symposium on Radio-Frequency Integration Technology (RFIT), Singapore, 2012, pp. 31-33, doi: 10.1109/RFIT.2012.6401604.

[63]. B. R. Rajesh and A. D. Sankar, "Cooling Strategies for Optimizing Thermal Performance in High-Load Cable Tunnels," IEEE Transactions on Industry Applications, vol. 54, no. 2, pp. 1038-1045, March/April 2018.

[64]. D. Zhu, J. Wang, C. L. Kok, L. Siek and Y. Zheng, "A new time-mode on-chip oscillator-based low power temperature sensor," 2015 IEEE International Conference on Electron Devices and Solid-State Circuits (EDSSC), Singapore, 2015, pp. 411-414, doi: 10.1109/EDSSC.2015.7285138.